Sensitivity Comparison of RFI Monitor Station and GBT L-Band Receiver
Electronics Division Technical Note No. 209

J. R. Fisher & Carla Beaudet

August 24, 2007

1 Introduction

A common problem with identifying sources of radio frequency interference (RFI) to radio telescopes is that the sensitivity of instruments used to find the direction and location of the RFI is often much poorer than the sensitivity of the telescope receivers and signal processors. A typical RFI search setup is a commercial spectrum analyzer, low-noise preamp, and a modest gain antenna that is less than 30 feet above ground.

In an effort to overcome this sensitivity disadvantage we have mounted a set of five antennas on the highest point of the GBT feed arm with two RF signal paths to the GBT equipment room via analog optical fiber links. The antennas, shown schematically in Figure 1, are mounted on a gimbal to keep them upright when the GBT is moved in elevation. Two directional antennas covering 105-1300 MHz and 1.2-1.7 GHz are mounted to two-axis positioners to control their azimuth and linear polarization orientation. The other three antennas are fixed, omnidirectional covering the bands 25-1300 MHz, 1.3-2.5 GHz, and 0.95-1.15 GHz. The first two are discones, and the third is a vertical array of co-linear dipoles optimized for the 960-1150 MHz DME aircraft navigation band. The electronics and positioner control logic for this RFI monitor station is described in [Fisher & Beaudet (2005)].

The primary purpose of the 0.95-1.15 GHz vertical array of co-linear dipoles is to make the pulse blanking technique described in [Fisher et al.(2005)] more effective by detecting pulses that are too weak to been seen individually in the GBT data but have an aggregate effect that can compromise the astronomical data at the DME frequencies. Because the DME pulses are short (about 5 μs) and widely spaced (typically 1 ms on average) they may be removed from the baseband-sampled data before Fourier transformation of the data into the frequency domain without seriously distorting the astronomical spectrum. The pulse-contaminated data sample values are set to zero. Less than 2% of the data are blanked at times when the DME signals are most numerous.

This note describes a comparison of sensitivities to DME RFI signals of the vertical array and the GBT L-band receiver near 1141 MHz, where their frequency ranges overlap.

2 Expected Sensitivities and Measurement Setup

The relative signal to noise (SNR) ratios for a signal received by the vertical array and the GBT L-Band receiver depends only on the system temperatures and the antenna gains in the direction of the signal source:

$$\frac{SNR_{va}}{SNR_{gbt}} = \frac{T_{gbt}G_{va}}{T_{va}G_{gbt}}, \tag{1}$$

where T_{gbt} and T_{va} are the system temperatures and G_{gbt} and G_{va} are the antennas gains of the GBT and vertical array, respectively. Roughly half of the vertical array's antenna pattern will see ground at 300 Kelvin, and its receiver noise measured at the antenna end of the transmission line to the preamp and power combiner is about 300 K so we assume $T_{va} = 450K$. The system temperature of the GBT

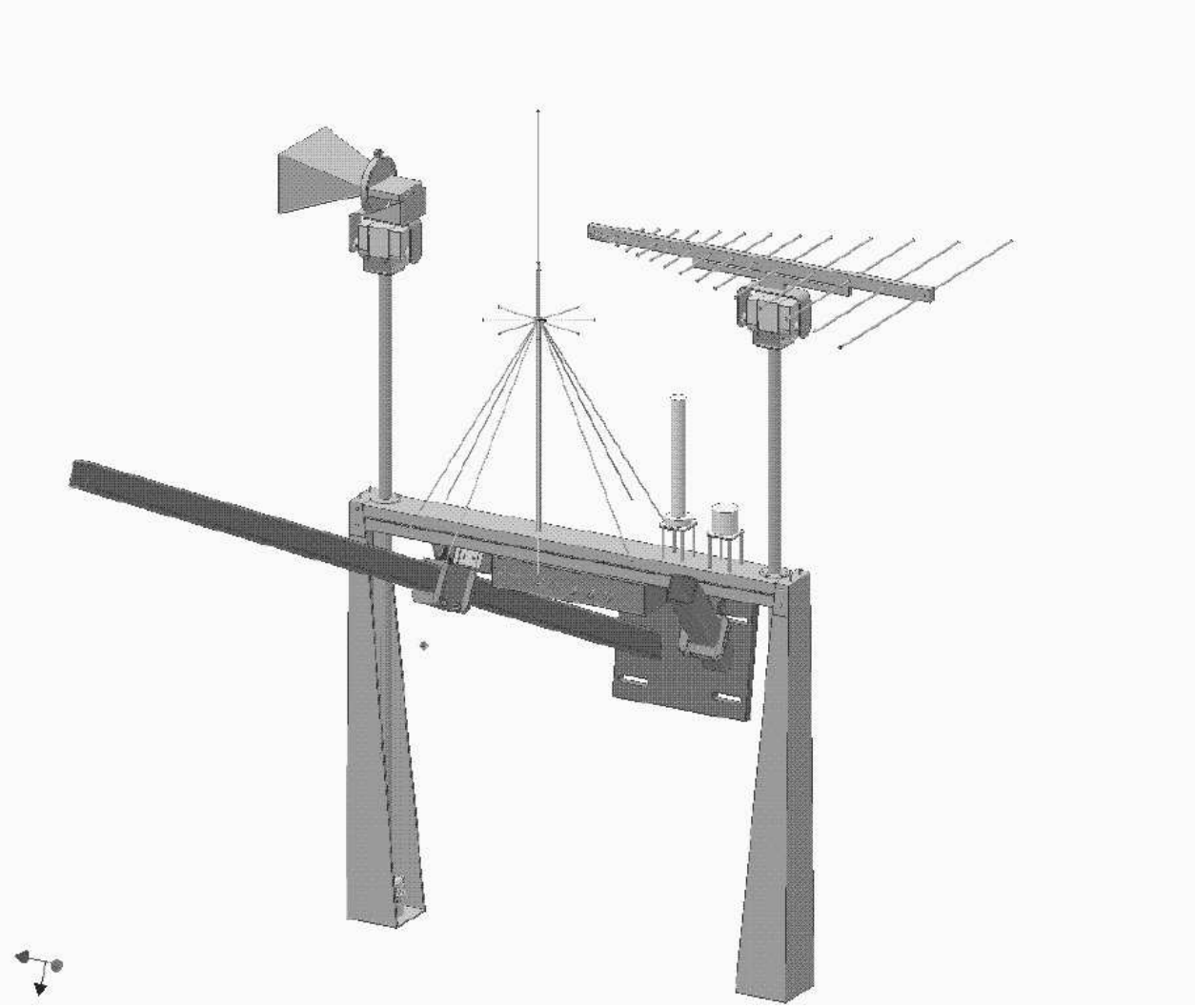

Figure 1: Schematic drawing of the antenna configuration on the one-axis gimbal at the top the GBT feed arm. From left to right, the antennas are the 1.2-1.7 GHz horn, the 25-1300 MHz discone, the 960-1150 MHz vertical dipole array, the 1.3-2.5 GHz discone, and the 105-1300 MHz log-periodic array. The azimuth rotators for the horn and log-periodic are at the bottom of the counterweights at the bottom of the figure.

L-Band receiver is about $T_{gbt} = 20K$. The broadside gain of one dipole is about 1.5 dB over isotropic (dBi) and four dipoles adds 6 dB, so the vertical array gain is about 7.5 dBi and $G_{va} = 5.6$. The GBT far-sidelobe gain will vary considerably over the sky, but let's assume a value of -15 dBi ($G_{gbt} = 0.03$) for directions more than about 40 degrees from the main beam. This is about 5 dB lower than the far-sidelobe gain typically assumed for a symmetric, blocked aperture antenna. Using these values,

$$\frac{SNR_{va}}{SNR_{gbt}} = \frac{20 \times 5.6}{450 \times 0.03} = 8.3 \tag{2}$$

Hence, the vertical array should have an 8:1 SNR advantage over the GBT far sidelobes. Closer to the GBT main beam, near the GBT reflector edge spillover directions, and at high elevations where the vertical array has lower gain, this advantage will be diminished considerably.

To test these assumptions we simultaneously recorded 5-MHz passbands centered on 1141.0 MHz from both the GBT and the vertical array using a dual-channel, 12-bit A/D PC-card (ADLink PCI-9812). The center 8 bits from this A/D were recorded at a rate of 10 mega-samples per second (MS/s). The GBT signal was converted to baseband with the normal GBT and spectral processor IF systems. The vertical array signal was converted to the 10-15 MHz second alias of the sampling rate and band-limited with a 11-14 MHz (3dB) final filter. These passbands provided unattenuated samples of the DME signal channels at 1140.0, 1141.0, and 1142.0 MHz. Each of these DME channels was isolated and optimally filtered with post-processing digital filters, and individual pulse arrival times and amplitudes were recorded as described in [Fisher et al.(2005)]. During this test the GBT was in access position with its main beam at a zenith distance of about 15 degrees. The L-band gregorian feed axis was nearly vertical so its peak spillover response at about +10 dBi described an annulus with a radius of 15 degrees around the zenith.

Fifteen data sets of one minute duration each were recorded at roughly five-minute intervals between 10:11 and 11:44 Eastern Daylight Time, August 14, 2007.

3 Results

Figures 2-4 show the distribution of SNR values for all pulses detected by both the GBT and the vertical array in three one-minute intervals at the beginning, near the middle, and at the end of the hour and a half data acquisition session. The SNR is defined as the ratio of the peak pulse power to the median noise power between pulses in the 0.25 MHz passband centered on a DME channel. A detection threshold of 15 times the median noise power was used to minimize false detections on random noise. Pulses coincident to within two microseconds in the GBT and vertical array channels were taken as detections of the same pulse, and only pulses paired with another pulse 12 microseconds later (a characteristic of DME transmissions) were recorded. An average of 23,000 pulses were counted in each one-minute interval.

The main characteristic of the distributions shown in Figures 2-4 is that nearly all of the pulses have a higher SNR in the vertical array channel. The distribution of GBT to vertical array pulse SNR ratios is shown in Figure 5. Three distributions are plotted to represent three pulse amplitude regions shown in Figure 6 to check for possible biases. The largest number of GBT to vertical array pulse SNR ratios fall around -13 dB, which is 5 dB lower than the expected value of -8 dB computed in Section 2. Figure 5 suggests that the median GBT sidelobe level is around -20 dBi, rather than the assumed -15 dBi, and varies from about -5 to -30 dBi well away from the main beam of the GBT. These numbers are subject to errors in the assumptions in Section 2. It's unlikely that any aircraft flew nearly overhead during data acquisition, where the GBT response would be high and the vertical array response relatively low. This is not a uniform sample of GBT far sidelobe directions, but the distribution of aircraft directions is reasonably representative.

Clusters of points in Figures 2-4 are probably from one aircraft or an overlap of of pulse clusters from a few aircraft. The horizontal banding of pulses may be due to aircraft running through many GBT sidelobe minima during the recording interval. The vertical array's response is expected to be fairly independent of direction of arrival. The smallest characteristic angular scale size of GBT sidelobes is

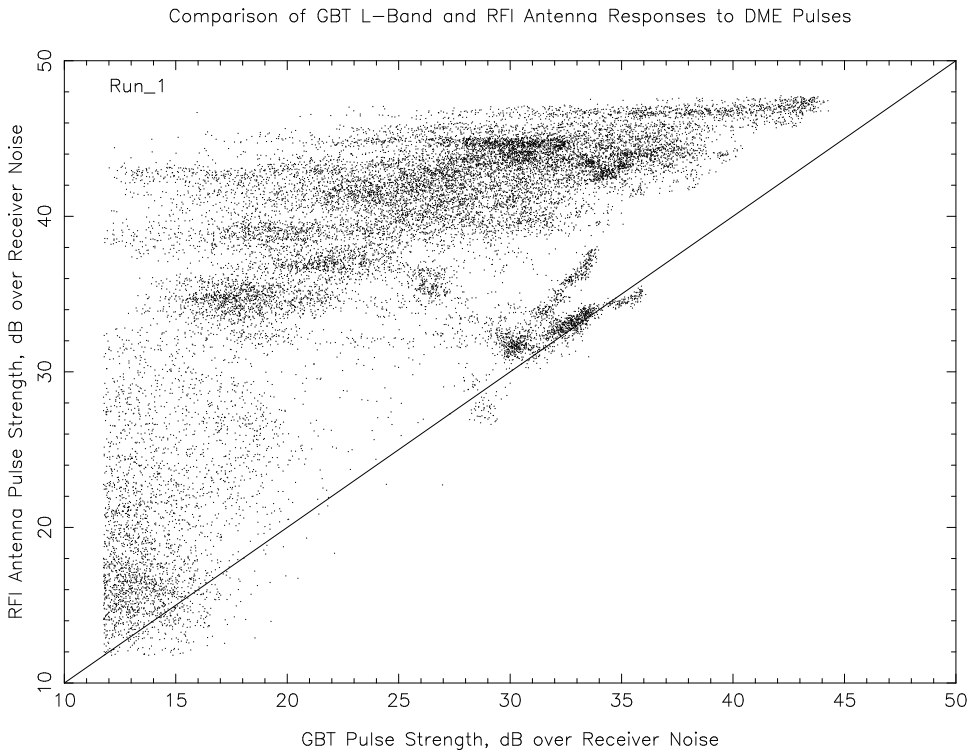

Figure 2: Distribution of pulses in the one-minute interval at 10:11 EDT as a function of measured GBT and vertical array pulse strength. Pulses very near the top of the scatter distribution are at or close to saturation of the vertical array data channel. A few GBT pulses at the top right corner are also near saturation. The left and bottom boundaries of the distribution show the chosen detection thresholds. The diagonal line is the locus of equal SNR in the GBT and vertical array channels.

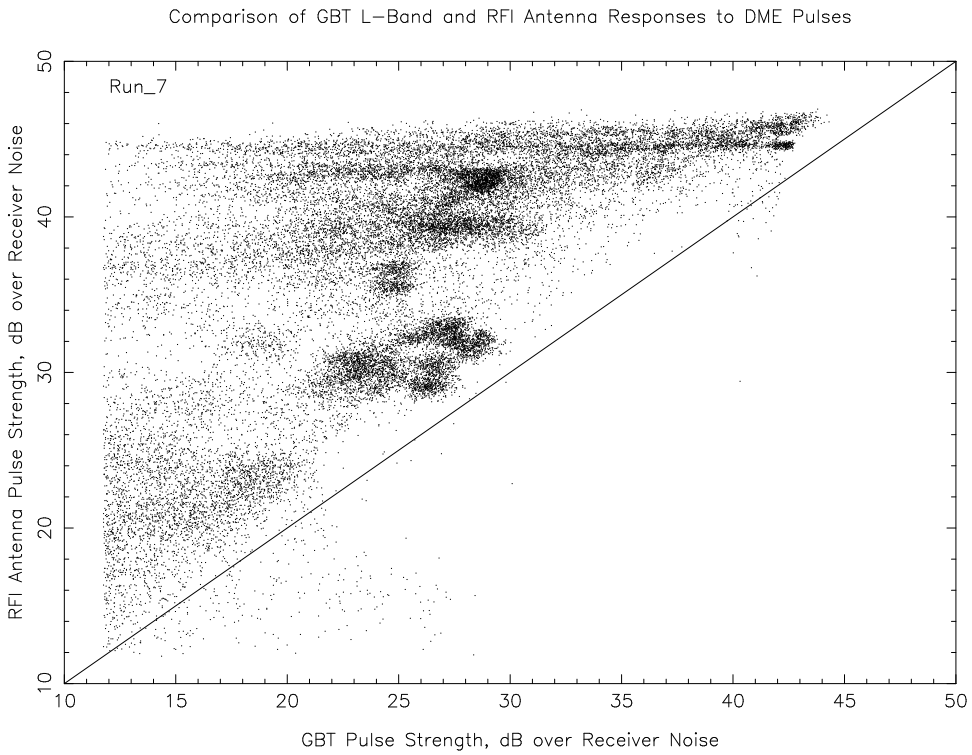

Figure 3: Same as Figure 2 for the one-minute interval at 11:00 EDT

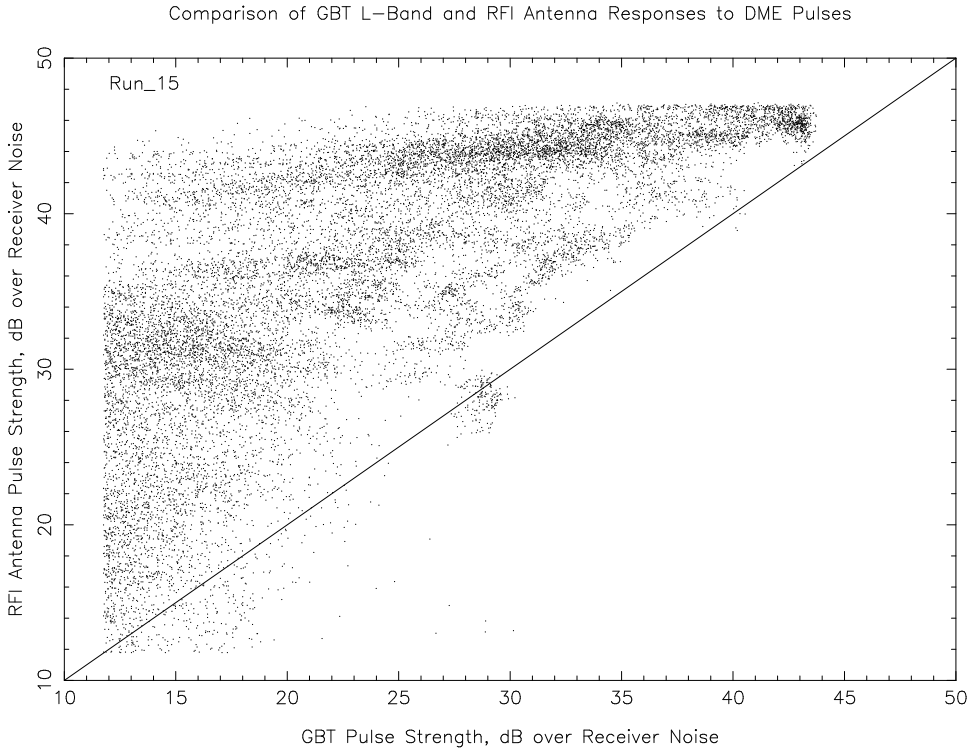

Figure 4: Same as Figure 2 for the one-minute interval at 11:44 EDT

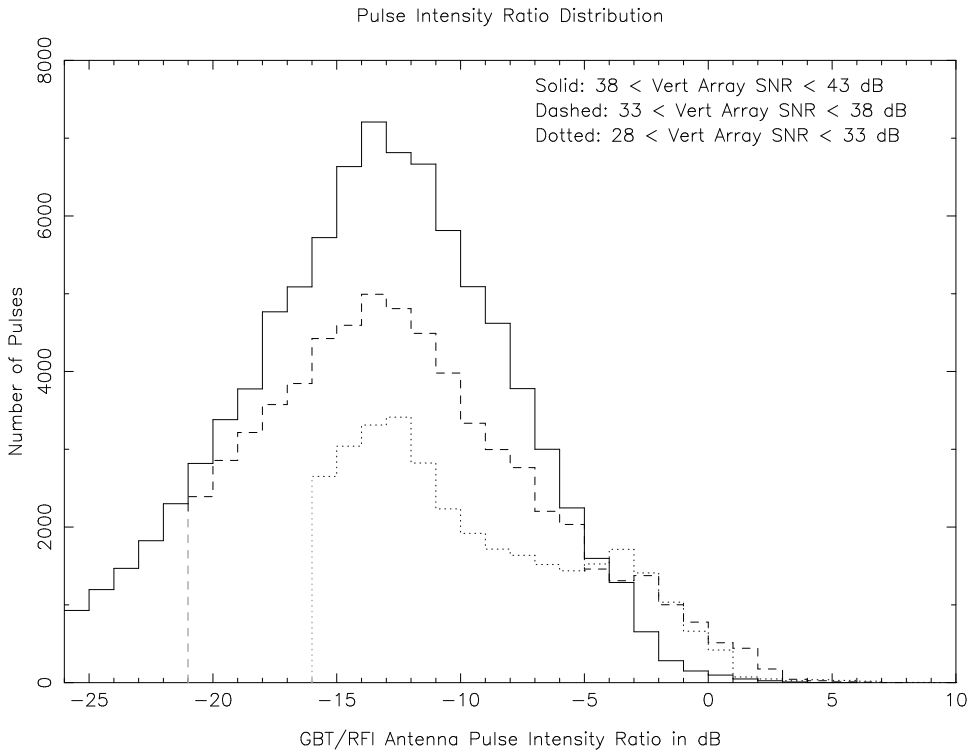

Figure 5: Distribution of (GBT SNR)/(Vertical Array SNR) for all coincident pulses recorded in the 15, one minute intervals that fell in the three areas shown in Figure 6.

about 10 arcminutes. An aircraft traveling with a lateral velocity component of 300 km/hr at a distance of 100 km would have an angular velocity of about three degrees per minute and pass through about 18 sidelobe minima in that minute.

Between 15 and 30% of the pulses recorded in the GBT data were not but should have been detected in the vertical array channel, based on the distributions shown in Figures 2-4. Our best guess is that these pulses are leaking through the unwanted sideband of the spectral processor IF system in the 5 MHz band adjacent to the intended band. The spectral processor sideband suppression is about 25 dB. Figure 7 shows the distributions of detected and undetected pulses in the vertical array channel as a function of GBT pulse SNR. Most of the undetected pulses are weak and consistent with a -25 dB leakage from unwanted sideband DME channels. The vertical array RF channel did not have a similar sideband leakage problem.

4 Conclusions

The measurements described in this report demonstrate that an RFI monitoring station can be implemented that has sensitivity equal to or greater than the far-sidelobe sensitivity of a modern low-noise radio telescope. The key design elements are signal processing capability comparable to radio astronomy back-ends in the RFI bandwidth of interest, antenna height equal to the height of the radio telescope, modest gain in the RFI monitor antenna, and reasonable pre-amplifier noise figure. The vertical array DME monitor antenna will provide enhanced sensitivity to pulse blanking techniques by allowing weaker pulses to be detected and blanked, as suggested in [Fisher et al.(2005)].

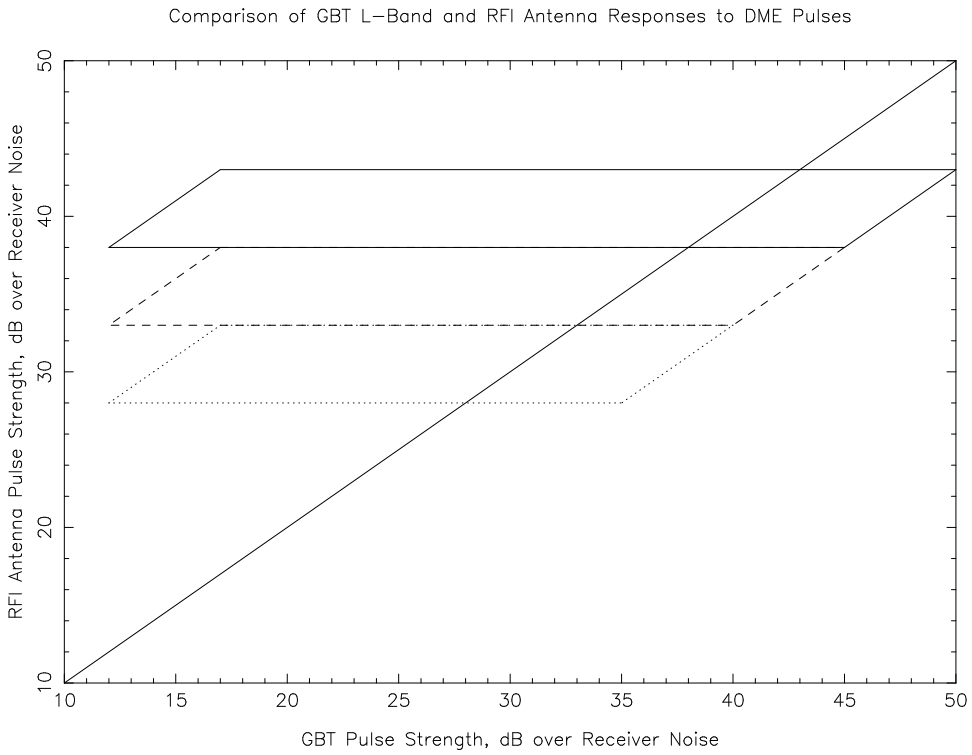

Figure 6: Boundaries of pulse locii whose distributions are shown in Figure 5. These boundaries apply to pulse distributions such as those shown in Figures 2-4. They were chosen to avoid pulse saturation regions and to give equal weight to GBT/Vertical Array SNR ratios at all pulse intensities within each area. Pulses on the right end of the top-most area would have been saturated in the GBT channel, but it is unlikely that any pulses would have fallen in this region in the absence of saturation.

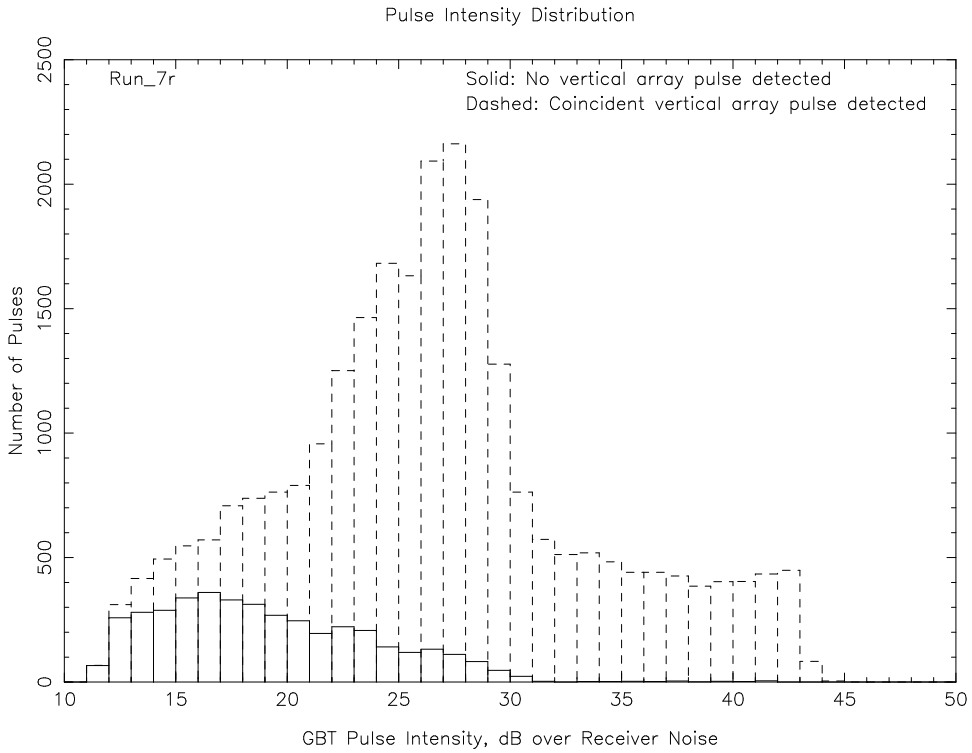

Figure 7: Distribution of GBT pulse SNR's for pulses that were detected and not detected in the vertical array antenna channel during the one-minute data set shown in Figure 3.

5 Acknowledgments

Thanks to Jeff Cromer for the mechanical design of the antenna mounting gimbal and to the Green Bank shop for fabrication. Thanks, too, to Bill Shank, Dave Woody, and Chuck Niday for electronics layout and assembly. Much of the hardware for the GBT monitor station was purchased with funds from NSF Grants 0079162 and 0420767.

References

[Fisher et al.(2005)] Fisher, J. R., Zhang, Q., Zheng, Y., Wilson, S. G., Bradley, R. F., 2005, Mitigation of Pulsed Interference to Redshifted HI and OH Observations between 962 and 1213 MHz, Astron J, vol. 129, pp2940-2949.

[Fisher & Beaudet (2005)] Fisher, J. R., Beaudet, C. 2005, Functional Description of PIC16F877A Functions and Interfaces to GBT RFI Monitor Station, NRAO Electronics Division Technical Note, No. 208, http://www.gb.nrao.edu/electronics/edtn/index.html